Heat and Mass Transfer Transients in Cylinder Drying: Part II. Felted Cylinders

A. H. NISSAN and H. H. GEORGE

Rensselaer Polytechnic Institute, Troy, New York

An investigation of transient heat transfer and water removal from a sheet on a steam cylinder was made. The sheet was pressed onto the cylinder by the aid of a felt. A theory describing the heat transfer in terms of the Fourier heat equation and appropriate boundary conditions was developed. The differential equation describing fluid flow in a capillary under the capillary potential was also developed. This equation was solved for small values of time.

The experimental work included the measurement of the transient temperatures at internal points in the sheet, the average felt temperature before and after a run, the mass of moisture lost by the sheet, and the mass of water gained by the felt.

It was found that on felted cylinders the majority of the moisture was removed by liquid transport. It was also found that heat was transferred through the sheet by vaporization-condensation cycles as well as conduction.

In Part I (5) heat and mass transfer transients on unfelted cylinders were discussed. As in previous work (4, 6) the problem of cylinder drying was divided into cycles, each of which is subdivided into four phases which are depicted in Figure 1. In this work interest is restricted to phase II; that is the sheet is on the cylinder and covered with a felt.

The function of the felt is threefold: to apply pressure to the sheet, beyond the latter's ability to withstand tension, in order to increase the heat transfer coefficient; to provide a source of capillary potential for abstracting water from the sheet; to act as a condenser for water vapor leaving the sheet. Of these three functions it is the last two that will be examined here.

In a series of papers (1, 4, 6) Nissan et al. derived a theory of cylinder drying using a system of approximate equations. In these papers the authors analyzed commercial paper making machines and found that the felt sometimes contributed substantially to the total drying. It was also shown that the felt effect was primarily the removal of liquid.

Brauns and Ponton (2) measured the ratio of liquid to vapor transport on an experimental paper machine and found that with sheets of initial water content of 0.43 lb. water/lb. solid on a felted cylinder about one-third of the total was due to liquid transport.

Smith and Atwood (8) have shown that the felt material is a significant variable. This would be expected owing to differences in thermal properties and pore structure. Nissan (4) has derived a parameter that shows the relative effectiveness of capillary suction. This parameter $(\gamma/\mu)^{1/2}$ is derived from an equation defining liquid movement in a capillary for large values of time which is later reduced to short time effects. This parameter will be rederived here for small values of time, a more tenable hypothesis in the case of cylinder drying.

There are three major mechanisms of heat and mass transfer from the sheet to the felt.

1. As the sheet goes onto the cylinder, a layer of air is trapped. This layer of air expands when heated by the cylinder. The expansion is enhanced by the formation of vapor at the surface. The vapor formation will be particularly important on cylinders above the boiling point. This expansion of the gas will be resisted by the wet sheet and a pressure results driving the liquid through the sheet. This mechanism was postulated as a major source of dewatering the sheet by Nissan (4).
2. When the felt, which is relatively dry compared with the sheet, contacts the sheet, capillary forces will be set up that will draw liquid into the felt. The temperature gradient in the sheet would tend to enhance this effect.
3. As the sheet progresses along the cylinder, the surface of the sheet away from the cylinder will become warmer and an increasing amount of vaporization will occur. This vapor will diffuse into the cooler felt and be condensed. The colder the felt the greater the amount of condensation. From this aspect therefore it is desirable to have felts of high specific heat.

THEORY

The amount of drying the sheet experiences depends on its temperature among other factors. This temperature is in turn dependent upon the rate of heat transfer through the surface. There are two mechanisms involved in the transfer of heat through the sheet: conduction and vaporization-condensation cycles.

Derivation of Conduction Heat Transfer Equations

A detailed derivation of the differential equations covering conduction is given in Part I (5). Briefly the derivation is as follows.

It is assumed that:

1. The felt and the sheet are isotropic.
2. The thermal properties are, to a first approximation, independent of temperature.
3. There are no internal heat sources or sinks.

Then the Fourier heat equation can be written as

$$\nabla^2 t = \frac{1}{\alpha}\frac{\partial t}{\partial \theta} \qquad (1)$$

If it is further assumed that

$$\frac{\partial^2 t}{\partial y^2} = \frac{\partial t}{\partial y} = 0$$

and that the distance traveled by an element of the sheet in the z direction is given by $z = z_o + V\theta$, then Equation (1) can be expressed as

$$\frac{\partial^2 t}{\partial x^2} + \frac{1}{V^2}\frac{\partial^2 t}{\partial \theta^2} = \frac{1}{\alpha}\frac{\partial t}{\partial \theta} \qquad (2)$$

Nissan and Hansen (5) have shown that if

$$\frac{\alpha^2 \pi^2 (2n+1)^2}{X^2 V^2} << 1 \qquad (3)$$

where n is an integer appearing in the series solution of Equation (1) and which does not usually exceed 2, then Equation (2) can reasonably be replaced by

$$\frac{\partial^2 t}{\partial x^2} = \frac{1}{\alpha}\frac{\partial t}{\partial \theta} \qquad (4)$$

In the problem of cylinder drying of paper or textile sheets this simplification is justified as the left-hand side of inequality (3) has a value of approximately 10^{-5}.

Before the problem is completely specified, it is necessary to define three boundary conditions. These conditions

TABLE 1. THE BOUNDARY VALUE PROBLEM FOR PHASE II

(1) The sheet

$$\frac{\partial^2 t}{\partial x_s^2} = \frac{1}{\alpha_s}\frac{\partial t}{\partial \theta} \qquad 4$$

$$t(x_s, o) = f_1(x_s) \qquad 4a$$

$$-k_s \frac{\partial t}{\partial x_s}\bigg|_{x_s=0} = h_1(t_s - t_{x_s=0}) \qquad 4b$$

$$-k_s \frac{\partial t}{\partial x_s}\bigg|_{x=X} = h_2(t_{x_s=X} - t_{x_f=0}) \qquad 4c$$

(2) The felt

$$\frac{\partial^2 t}{\partial x_f^2} = \frac{1}{\alpha_f}\frac{\partial t}{\partial \theta} \qquad 4$$

$$t(x_f, o) = f_2(x_f) \qquad 4d$$

$$-k_f \frac{\partial t}{\partial x_f}\bigg|_{x_f=0} = h_2(t_{x_s=X} - t_{x_f=0}) \qquad 4e$$

$$-k_f \frac{\partial t}{\partial x_f}\bigg|_{x_f=\delta} = h_3(t_{x_f=\delta} - t_a) \qquad 4f$$

TABLE 2. THE DIMENSIONLESS GROUPS

$$r = \frac{x_s}{X}$$

$$f = \frac{x_f}{\delta}$$

$$R_1 = \frac{h_1 X}{k_s}$$

$$R_2 = \frac{h_2 X}{k_s}$$

$$R_3 = \frac{h_2 \delta}{k_f}$$

$$R_4 = \frac{h_3 \delta}{k_f}$$

$$\tau_s = \frac{\alpha_s \theta}{X^2}$$

$$\tau_f = \frac{\alpha_f \theta}{\delta^2}$$

consist of specifying the initial temperature distribution and the heat flux conditions at both surfaces.

The same equations, (1) to (4), apply in phase II, but here there are two regions adjoining each other with a plane of finite thermal resistance between them. The boundary conditions must therefore be defined for both regions. The two boundary-value problems thus defined are not independent as they are coupled together through the common boundary condition at their interface.

The complete boundary value problems are presented in Table 1.

Similar but simpler problems were examined in the literature (3). The analytical solutions presented for the similar problems were of open form and of such complexity as to render them almost useless for massive calculations. Furthermore h_2 in 4c is likely to be a complicated function of mass transfer and other factors at the interface.

For these reasons recourse was made to a numerical solution employing a set of finite difference equations.

At this point it was convenient to reduce the problem to a dimensionless form with the dimensionless groups presented in Table 2.

The finite difference equations can be deduced directly from the definitions of first and second derivatives by dropping the limiting operation. The finite difference equations thus derived are listed in Table 3.

It is also of interest to calculate the heat fluxes across each face, particularly to and from the felt:

$$Q_1 = \frac{R_3}{t_B}\sum_{\tau_{start}}^{\tau_{max}} (t_{r=1} - t_{f=0})\,\Delta\tau_f$$

flux to felt (13)

$$Q_2 = \frac{R_4}{t_B}\sum_{\tau_{start}}^{\tau_{max}} (t_{f=1} - t_a)\,\Delta\tau_f$$

flux from felt (14)

TABLE 3. THE FINITE DIFFERENCE EQUATIONS

(A) For the sheet

$$t_{(r,\,\tau_s+\Delta\tau_s)} = \frac{t_{(r+\Delta r,\,\tau_s)} + t_{(r-\Delta r,\,\tau_s)} + \left[\dfrac{\overline{\Delta r^2}}{\Delta\tau_s} - 2\right] t_{(r,\,\tau_s)}}{\dfrac{\overline{\Delta r^2}}{\Delta\tau}} \qquad (5)$$

when $0 < r < 1$

$$t_{(0,\,\tau_s+\Delta\tau_s)} = \frac{R_1 t_s + (1/\Delta r)\,t_{(\Delta r,\,\tau+\Delta\tau_s)}}{R_1 + 1/\Delta r} \qquad (6)$$

$$t_{(1,\,\tau_s+\Delta\tau_s)} = \frac{R_2 t_{(f=1,\,\tau_f+\Delta\tau_f)} + (1/\Delta r)\,t_{(1-\Delta r,\,\tau_s+\Delta\tau_s)}}{R_2 + 1/\Delta r} \qquad (7)$$

(B) For the felt

$$t_{(f,\,\tau_f+\Delta\tau_f)} = \frac{t_{(f+\Delta f,\,\tau_f)} + t_{(f-\Delta f,\,\tau_f)} + \left[\dfrac{\overline{\Delta f^2}}{\Delta\tau_f} - 2\right] t_{(f,\,\tau_f)}}{\overline{\Delta f^2}/\Delta\tau_f} \qquad (8)$$

when $0 < f < 1$

$$t_{(f=0,\,\tau_f+\Delta\tau_f)} = \frac{R_3 t_{(r=1,\,\tau_s+\Delta\tau_s)} + (1/\Delta f)\,t_{(\Delta f,\,\tau_f+\Delta\tau_f)}}{R_3 + 1/\Delta f} \qquad (9)$$

$$t_{(f=1,\,\tau_f+\Delta\tau_f)} = \frac{R_4 t_a + (1/\Delta f)\,t_{(1-\Delta f,\,\tau_f)}}{R_4 + 1/\Delta f} \qquad (10)$$

Solving Equations (7) and (9) simultaneously one gets

$$t_{(r=1,\,\tau_s+\Delta\tau_s)} = \frac{\left[\left(\dfrac{1/\Delta r}{R_2}\right) t_{(1-\Delta r,\,\tau_s+\Delta\tau_s)} + \left(\dfrac{1/\Delta f}{R_3 + 1/\Delta f}\right) t_{(\Delta f,\,\tau_f+\Delta\tau_f)}\right]}{\left[\dfrac{R_2 + 1/\Delta r}{R_2} - \dfrac{R_3}{R_3 + 1/\Delta f}\right]} \qquad (11)$$

and

$$t_{(f=0,\,\tau_f+\Delta\tau_f)} = \frac{\left[\left(\dfrac{1/\Delta f}{R_3}\right) t_{(\Delta f,\,\tau_f+\Delta\tau_f)} + \left(\dfrac{1/\Delta r}{R_2 + 1/\Delta r}\right) t_{(1-\Delta r,\,\tau_s+\Delta\tau_s)}\right]}{\left[\dfrac{R_3 + 1/\Delta f}{R_3} - \dfrac{R_2}{R_2 + 1/\Delta f}\right]} \qquad (12)$$

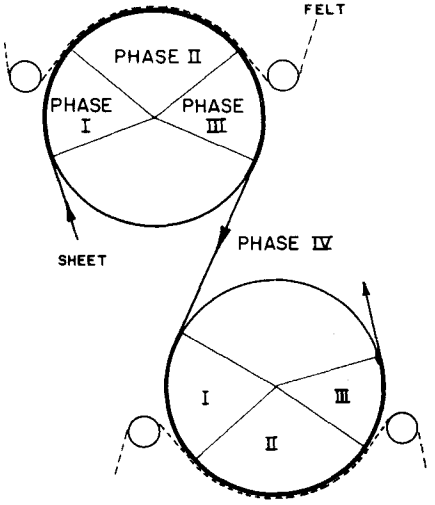

Fig. 1. The four phases in a cycle of hot cylinder drying when a felt is used.

$$Q_3 = \frac{R_1}{t_B} \sum_{\tau\text{start}}^{\tau\max} (t_s - t_{\tau=0})\,\Delta\tau_s$$

flux to sheet (15)

It should be noted that Q_1, Q_2, and Q_3 are dimensionless heat fluxes where t_B is introduced for this reason.

Equations (5) through (15) are directly solved by simple substitutions. These equations were programed for an IBM-650 digital computer.

Inherent in the finite difference equations are some parameters through which the physical properties enter. The process of reducing the equations to dimensionless form has assigned a value of one to the thermal resistance of each of the two regions, that is the sheet and the felt. The surface conditions are then ratios of surface resistance to internal resistance.

The modulus $\left| \frac{\overline{\Delta r^2}}{\Delta\tau_s} - 2 \right|$ must be greater than zero in order that the finite difference equation be stable and thus that the numerical solution of the finite difference equation be a reasonable approximation to the solution of the partial differential equation. In choosing values of the moduli there is only one degree of freedom; that is once one has chosen a value for one region, the value in the other region is fixed by the geometry and thermal properties of the system. Expressing the two moduli in dimensional terms and equating the time increments one obtains

$$(M_f + 2) = \left(\frac{\overline{\Delta f^2}}{\overline{\Delta r^2}}\right)\left(\frac{\delta^2}{\overline{X}^2}\right)\left(\frac{\alpha_s}{\alpha_f}\right)(M_s + 2) \qquad (16)$$

The difference in properties of the two regions also manifests itself in the interface Nusselt numbers R_2 and R_3. There is a single-valued heat transfer coefficient h_2 governing the heat transfer at the interface. However when this is reduced to a Nusselt number hX/k, care must be used in defining this ratio, since the value depends on the region to which it is being referred. These values of R_2 and R_3 are interrelated by the conductivity and thickness of the two regions, and equating the definitions of R_2 and R_3 through their common value of h_2 one finds

$$R_3 = \left(\frac{k_s}{k_f}\right)\left(\frac{\delta}{X}\right) R_2 \qquad (17)$$

Derivation of the Capillary Equation

When a liquid flows through a passage under a capillary potential head it is subject in general to three forces: gravitational, frictional, and capillary. These forces can all be expresed analytically and substituted into Newton's second law:

$$\frac{1}{g_c}\Sigma F \propto \frac{\partial}{\partial\theta}\left(\rho a H \frac{dH}{d\theta}\right) \qquad (18)$$

The gravitational force acting on the liquid in the capillary passage is

$$\frac{1}{g_c} Fg = \rho\, aHg \sin\phi \qquad (19)$$

In small capillary passages the frictional forces can become large. In these small passages the flow of liquid can be assumed to be laminar. The average fluid velocity for a passage of constant cross section can be expressed as

$$\bar{u} = \frac{m^2}{\mu k_K} \cdot \frac{\Delta P}{g_c L} \qquad (20)$$

where k_K = approximately 3 for fibrous structures (7).

In view of the above the frictional force can be written as

$$\frac{1}{g_c} F_f = \frac{3\mu a}{m^2} H \frac{dH}{d\theta} \qquad (21)$$

The capillary force is simply

$$F_c = S\,\gamma\cos\Psi \qquad (22)$$

Substituting Equations (19), (21), and (22) into Equation (18) one obtains the general differential equation of flow under a capillary potential:

$$\left(\frac{1}{g_c} S\gamma\cos\Psi\right) - \left(\frac{3\mu a}{m^2} H\frac{dH}{d\theta}\right) - (\rho\, a\, H\, g \sin\phi) = \frac{d}{d\theta}\left(\rho a H \frac{dH}{d\theta}\right) \qquad (23)$$

Equation (23) is not readily solvable as it is both nonhomogeneous and nonlinear. A solution may be effected for large values of time by considering the right-hand member to be negligible. This has been done by Palmer (7). In the present work a solution for small values of time is desired. This may be done as follows.

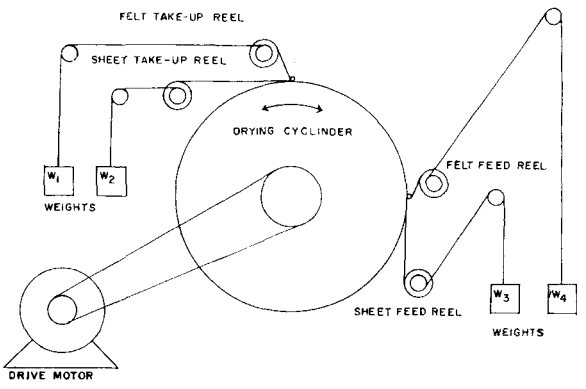

Fig. 2. Schematic drawing of apparatus.

At small values of time the gravitational force is small as it is directly proportional to the height of liquid in the passage. If the gravitational term is neglected, Equation (23) becomes linear and first order with respect to the variable $v = H(dH)/(d\theta)$. This approach leads to the solution

$$H = \left\{\frac{2A}{B}\left[\theta - \frac{C}{B}\left(e^{-\frac{B}{C}\theta} - 1\right)\right]\right\}^{1/2} \qquad (24)$$

where

$$A = \frac{\gamma\cos\Psi}{g_c\,\rho g m \sin\phi}$$

$$B = \frac{3\mu}{\rho m^2 g \sin\phi}$$

$$C = \frac{1}{g\sin\phi}$$

For a system of fine pores $C/B << \theta$, and Equation (24) reduces to

$$H = \left(\frac{2A}{B}\theta\right)^{1/2} \qquad (25)$$

which is identical with the result obtained by Nissan through another route. Thus for a given set of sheet, felt, and liquid at different temperatures H is proportional to $(\gamma/\mu)^{1/2}$.

Liquid Fraction of Felt Moisture Gain

When the felt is in contact with the sheet, it extracts moisture from the sheet. This transport occurs in both the liquid and vapor phases. The relative magnitude of the two mechanisms can be evaluated from mass and energy balances.

The total heat transferred to the felt is

$$Q_T = M\,\bar{c}_p\,(t_2 - t_1) \qquad (26)$$

Q_T is the sum of the heat transferred by conduction and moisture transport:

$$Q_V = (1-\eta)\xi\lambda$$

$$Q_L = \eta\, C_{PL}\xi\,(\bar{t}_t - t'_{s_0})$$

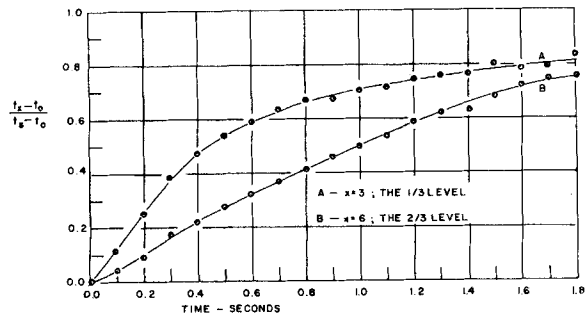

Fig. 3. Accomplished temperature vs. time at distances of 1/3 and 2/3 of the sheet thickness from the cylinder.

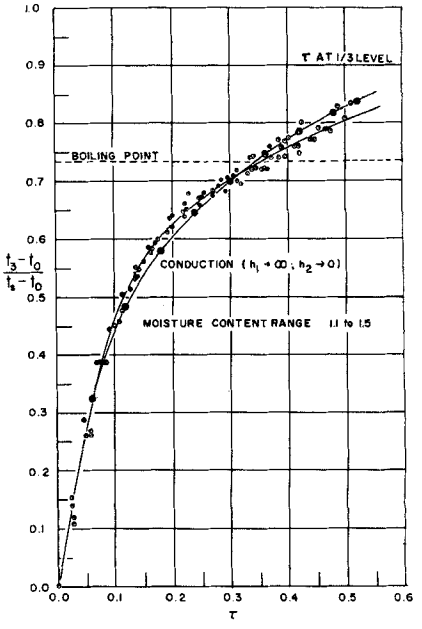

Fig. 4. Accomplished temperature vs. dimensionless time parameter τ at distance of 1/3 sheet thickness from the cylinder surface.

t_1, t_2, and t'_{s_o} are measurable temperatures, whereas $\bar{t}_t$ is not readily so. Define

$$\bar{t}_t = \frac{\int_o^\tau t d\tau}{\int_o^\tau d\tau} = \frac{\int_o^\tau t d\tau}{\tau} \qquad (27)$$

The right-hand member of Equation (27) can be evaluated graphically from the solutions of Equations (5) through (12). The conduction contribution to Q_τ can be estimated from the numerical solutions at the proper values of R_1 and R_2.

DESCRIPTION OF APPARATUS

In this study of felted cylinder driers experiments were performed on a single cylinder drier. The drier is basically the machine described by Nissan and Hansen (5). The machine was modified to accommodate a drier felt. The drier is shown schematically in Figure 2.

EXPERIMENTAL PROCEDURE

A sample sheet, 1 m. long, was prepared by stitching three layers of bleached muslin cloth together. Five thermocouples (0.001-in. copper-constantan) were placed between each sheet with the junctions placed at the middle of the cross direction. The leads of the couples were taken to the edges of the sample and connected to 30-gauge lead wires. These lead wires were run down the edge of the sheet to the end.

Mylar plastic leads were attached to each end of the sample. These plastic leads served two functions; they got the samples on and off the cylinder, and they covered the hot sheet to cut down on evaporation losses.

The felt sample was cut from a 3,000 g./sq. m. woolen paper-making felt. The felt sample was made somewhat longer than the sheet sample in order to insure that the sheet was completely covered. A single iron-constantan thermocouple was sewn on the open side of the felt in order to measure the average temperature of the felt on the roll.

The sheet and felt samples were both placed on rolls and placed on the drier as shown in Figure 2. Before the samples were passed over the hot cylinder, the initial reading of two sheet thermocouples were recorded as was the initial felt temperature. The samples were then passed over the hot surface and wound up on the take-up reels. During the pass the transient sheet temperatures were recorded. Immediately after the pass the thermocouple in the felt was attached to the recording potentiometer. The samples were wrapped in aluminum foil to prevent radiation from the cylinder surface, as this was found to have a marked effect on the average felt temperature. When the sheet had cooled to 100°F., the cylinder rotation was reversed and the samples were returned to the feed reels. The same measurements were made on the reverse pass as on the forward pass. After the reverse pass both samples were removed and weighed. This cycle was repeated until the sheet reached a moisture content of 1.00 lb. water/lb. solid. The sheet was then rewetted and allowed to stand overnight before the run was repeated.

EXPERIMENTAL RESULTS

Temperature Measurements

A series of six experiments were performed over a moisture ratio range of 1.00 to 1.65 lb. of water/lb. of solid. The experiments were performed on a three-ply muslin sample. The operating conditions are summarized in Table 4.

It was found that the temperature was dependent on both time and sheet moisture content. In order to show the effect of sheet moisture content the data were treated by a linear regression to obtain a family of straight lines of accomplished temperature change as a function of moisture content with time as a parameter. It was then shown that the use of a linear regression was valid at the 95% confidence level. These results were then cross plotted to give accomplished temperature change as a function of time. A typical curve is shown in Figure 3.

Table 4. Conditions for Temperature Experiments

Sample material:	Three-ply muslin composite
Dry thickness:	0.036 in.
Areal density:	0.102 lb./sq. ft.
Void volume:	56%
Contact length:	11.75 in.
Cylinder speed:	8.75 rev./min.
Cylinder surface temperature:	225° ± 3°F.
Ambient temperature:	80 to 90°F.
Tension on sheet:	1.88 lb.$_f$/in. of width
Felt surface density:	3000 g./sq. m.

The data were also plotted as accomplished temperature change against the Fourier modulus, as shown in Figures 4 and 5. The curves labeled conduction were calculated by use of the finite difference equations previously developed. R_1 was made large, that is h_1 approaching infinity, and R_2 was set at a very low value, that is h_2 approaching zero. The data taken at the 1/3 level (1/3 the thickness of the sheet from the cylinder surface) lie on a single curve that agrees with the conduction curve. The data at the 2/3 level, or 2/3 the thickness of the sheet from the surface of the cylinder, all lie above the conduction curve, indicating that there is some additional mechanism for heat transfer. The second mechanism becomes more pronounced as the moisture content increases.

Weight Data

The felt moisture gain was measured over a range of sheet moisture contents at three cylinder temperatures. The smoothed data are shown in Figures 6 and 7. The data for room-temperature runs are presented in Figure 6. These data were the most consistent moisture-gain data obtained owing to the negligible evaporation losses. This consistency made it possible to show a significant correlation of the effect of felt moisture content. The data at elevated

temperatures are plotted in Figure 7 along with the 90% confidence limits of the least-squares line through the data. Both sets of data were checked for correlation between felt moisture content and felt gain, and in each case a very weak correlation was found. A multivariable linear regression was performed on each set, and it was found that the entire family of curves lay within the 90% confidence band of the two variable regressions. In view of the foregoing result it was concluded that the correlation of felt moisture content on felt gain was not significant for the range of moisture content reported here.

Liquid-Transport Fraction

The fraction of total water entering the felt as a liquid was calculated from the moisture-gain data and the felt temperature change. The resulting values of η were scattered and the 90% confidence limits large, particularly for the 225°F. run. The 90% confidence limits do not overlap, and hence there is a significant difference in the two runs. These data are plotted in Figure 8. As in the case of the weight-loss data the partial correlation between felt moisture and η was not significant for the range of felt moisture content used in this study.

DISCUSSION

In the theory section four mechanisms were mentioned: vaporization-condensation cycles in the sheet, condensation of vapor in felt, capillary suction moisture transport, and pressure gradient due to expanding air film at closed surface.

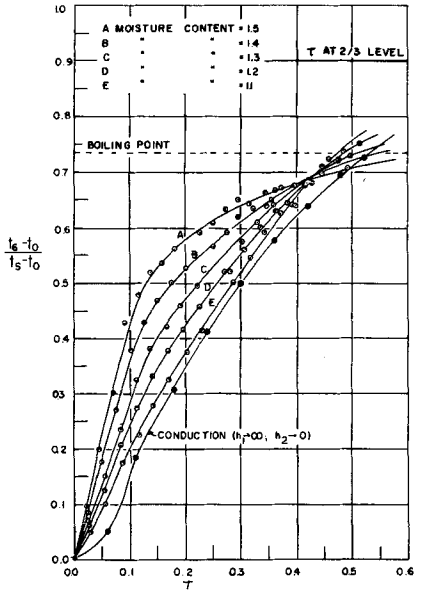

Fig. 5. Accomplished temperature vs. dimensionless time parameter τ at distance of 2/3 sheet thickness from the cylinder surface.

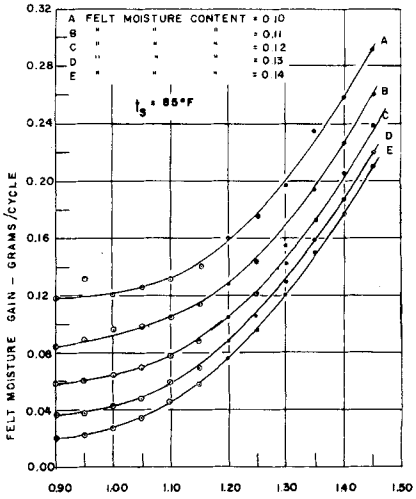

Fig. 6. Felt moisture gain vs. sheet moisture content at 85°F. cylinder temperature.

Vaporization-Condensation Cycles in the Sheet

The temperatures at the 1/3 level, that is 1/3 of the thickness of the sheet from cylinder surface, all lie in a single curve that falls close to the pure conduction curve. There are however some significant differences. From $\tau \cong 0.1$ to $\tau \cong 0.38$ the experimental results lie somewhat above the pure conduction curve; for $\tau > 0.38$ the experimental results are a little low. For $\tau < 0.38$ the temperature is below the boiling point, and some vapor is condensing as it is forced up to this level by expansion. The condensation, as well as the conduction heating, increase the temperature of the sheet at this level. When the temperature reaches the boiling point, vaporization takes place, causing the sheet now to heat more slowly than it would with pure conduction.

The temperatures at the 2/3 level, that is 2/3 of the thickness of the sheet from cylinder surface, are dependent upon the moisture content of the sheet. The curves all come together at $\tau = 0.44$, about the time the sheet leaves the cylinder. In all cases the actual temperatures are greater than the pure conduction temperature but never reach the boiling point, indicating that there is net condensation at this level.

As the temperatures increase, they first increase in deviation from the conduction line; as they approach the boiling point, the deviation decreases, indicating a decrease in the amount of condensation as the driving force for condensation decreases.

These data were for cylinders above the boiling point. Nissan and Hansen (5) found little indication of vaporization-condensation on cylinders below the boiling point. At high moisture contents the experimental temperatures exceeded the zero surface resistance conduction temperatures by about 3°F. This value of 3°F. is only slightly outside the 95% confidence band of their data, indicating that the convection effect is very small.

Condensation of Vapor in the Felt

The amount of liquid condensed in the felt is represented by the difference between the total gain lines and the total liquid gain lines in Figures 9 and 10. The relative importance of vaporization increases with increasing surface temperature and decreasing moisture content. The higher the surface temperature the higher the temperature throughout the sheet and particularly near its outer surface. This higher temperature means a greater vapor concentration in the atmosphere adjacent to the felt-sheet interface and hence a greater mass of condensed vapor.

The relative importance of vapor condensation decreases with increasing sheet moisture content, but the amount of vapor condensed is about the same. In both experiments the absolute amount of condensation increased slightly, but in view of the scatter in η (see Figure 8) this trend is not significant.

Figure 5 shows the temperature in the sheet at the 2/3 level. The average temperature during a pass increases with increasing moisture content; hence the rate of evaporation should increase. It is apparent that one cannot use the temperature results at the 2/3 level to correlate what occurs at the outer surface of the sheet, that is the sheet-felt interface, in view of the large change in behavior between the 1/3 and 2/3 levels.

Capillary Suction Moisture Transport

In the theory section it was shown that the rate of liquid extraction should be directly proportional to the parameter. $(\gamma/\mu)^{1/2}$. This parameter was used to calculate the capillary moisture transport at elevated surface temperatures from the results obtained at room temperatures.

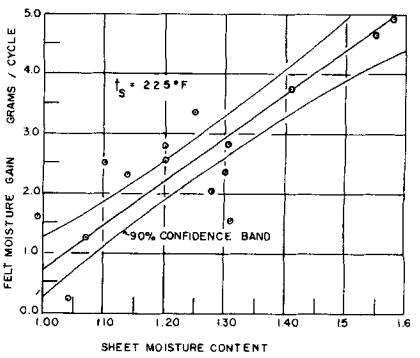

Fig. 7. Felt moisture gain vs. sheet moisture content at 225°F. cylinder temperature.

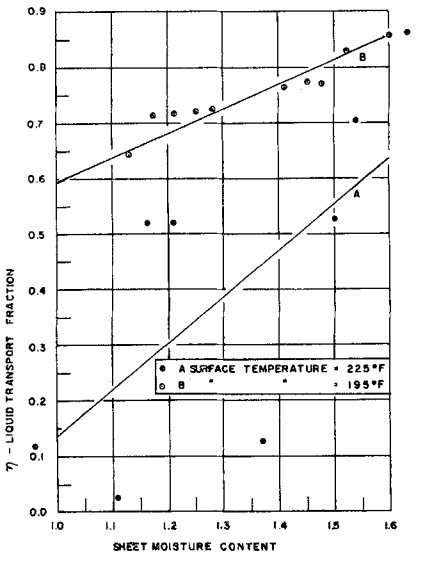

Fig. 8. Liquid transport fraction of total moisture gained by felt vs. sheet moisture content.

Capillary suction was the only mechanism causing the felt to pick up water at room temperature. These results are shown on Figure 6. To obtain values at higher temperatures results taken from Figure 6 were multiplied by the ratios of the parameters $(\gamma/\mu)^{1/2}$ obtained at the two temperatures.

The change in capillary flow is small. The parameter $(\gamma/\mu)^{1/2}$ changes about 2% between 195° and 225°F. and from 85°F. the change is roughly 20%.

For the materials used and the moisture content ranges investigated the effect of capillary suction is relatively small. However for systems with greatly different pore sizes and felts of high wettability the effect could be large.

Pressure Gradient Due to Expanding Air Film

The remaining transport of liquid is a result of the pressure gradient produced by the heating up of the trapped air layer. This mechanism does not occur when the entire system is at ambient temperature; thus the liquid transport occurring in the room-temperature runs is due entirely to capillary suction. When the cylinder is below the boiling point, the trapped air will gain water vapor until it is in equilibrium with the surrounding sheet. When equilibrium is reached, vapor will cease to be formed and the pressure driving force will be correspondingly limited. When the cylinder is above the boiling point, the rate of vapor formation is limited only by the rate of heat transfer. The pressure driving force is not limited, as vapor can continue to form as long as liquid is present. Thus the effect of the expanding gas film will be much greater when the cylinder temperature is above the boiling point.

In Figures 9 and 10 the expanding film effect is represented by the distance between the capillary liquid-gain and total liquid-gain lines. It will be noted that in both experiments this effect increases with increasing sheet moisture content. The more water there is in the sheet the less chance there is for the trapped gas film to blow through the sheet, and hence a greater portion of the available pressure energy goes toward moisture movement.

CONCLUSION

1. The existence of vapor-condensation cycles within the sheet was shown for cylinder surface temperatures greater than the boiling point.
2. The drying that occurs during Phase II for the range of conditions studied was primarily due to liquid transport. The effect of vapor transport increased with increasing surface temperature.
3. Liquid transport was due mainly to trapped gas pressure gradients and secondarily to capillary suction.
4. The effect of the trapped gas film was appreciable and increased in magnitude with increasing surface temperature and sheet moisture content.
5. The capillary suction effect was found to be small for the materials and conditions used. The magnitude of this effect, for a given system, was shown to increase with increasing sheet moisture content and decreasing felt moisture content.
6. An increase in drying of nearly threefold was observed by increasing the surface temperature beyond the boiling point. This threefold increase was noted between 195° and 225°F.

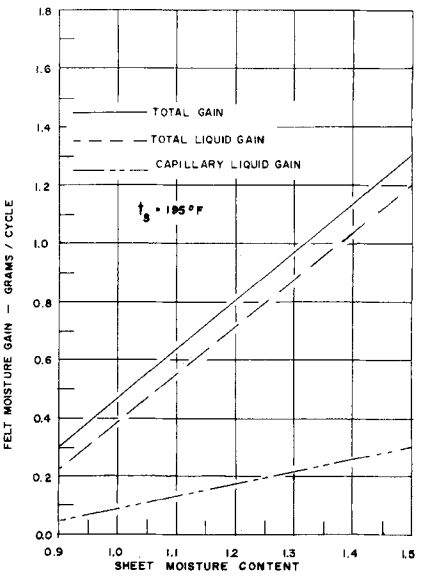

Fig. 9. Division of total gain by felt into vapor gain, total liquid gain, and capillary liquid gain at surface temperature of 195°F.

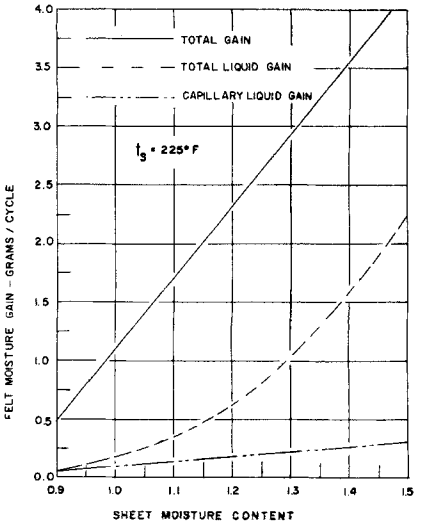

Fig. 10. Division of total gain by felt into vapor gain, total liquid gain, and capillary liquid gain at surface temperature of 225°F.

NOTATION

A = $\gamma \cos \theta / g_c \rho g m \sin \phi$ equilibrium height in a capillary, ft.
A_n = general term of an alternating series
a = cross-sectional area of a capillary, sq.ft.
B = $3\mu/\rho m^2 g \sin \phi$, hr./ft.
C = $1/g \sin \phi$, hr.²/ft.
C_p = specific heat, B.t.u./lb.-°R.
C_{P_L} = specific heat of liquid water, B.t.u./lb.-°R.
ΣF = total force, lb.$_{(f)}$
F_c = capillary force, lb.$_{(f)}$
F_f = frictional force, lb.$_{(f)}$
F_g = gravitational force, lb.$_{(f)}$
f = relative distance in felt from sheet-felt interface, dimensionless
f_1, f_2 = boundary value functions (1), (2)
g = acceleration due to gravity, ft./hr.²
g_c = conversion factor, lb.$_m$ ft./lb.$_f$ hr.²
H = height of capillary, ft.
h_1 = cylinder to sheet heat transfer coefficient, B.t.u./sq.ft.-°R. hr.
h_2 = sheet to felt heat transfer coefficient, B.t.u./sq.ft.-°R. hr.
h_3 = felt to air heat transfer coefficient, B.t.u./sq.ft.-°R. hr.
k = thermal conductivity, B.t.u./ft.-°R. hr.
k_K = shape factor in Kozeney's equation
M = mass, lb.$_m$
M_f = modulus of felt, $\left[\frac{\overline{\Delta f^2}}{\Delta \tau_f} - 2\right]$ dimensionless
M_s = modulus of sheet, $\left[\frac{\overline{\Delta r^2}}{\Delta \tau_s} - 2\right]$, dimensionless
m = mean hydraulic depth, ft.
n = integer

$\Delta P/L$ = pressure drop per unit length, lb.$_{(f)}$/cu. ft.
Q_T = total heat flux across an interface, B.t.u./hr. sq.ft.
Q_L = heat flux to felt through liquid transport, B.t.u./hr. sq.ft.
Q_V = heat flux to felt through vapor transport, B.t.u./hr. sq.ft.
Q_1 = dimensionless heat flux between sheet and felt, dimensionless
Q_2 = dimensionless heat flux between felt and air, dimensionless
Q_3 = dimensionless heat flux between surface and sheet, dimensionless
q = heat flux, B.t.u./hr. sq.ft.
R_1 = Nusselt modulus based on h_1, dimensionless
R_2 = Nusselt modulus based on h_2 and sheet properties, dimensionless
R_3 = Nusselt modulus based on h_2 and felt properties, dimensionless
R_4 = Nusselt modulus based on h_4, dimensionless
r = relative distance in sheet from cylinder, dimensionless
S = perimeter of capillary, ft.
t = temperature, °R.
t_B = base temperature on an absolute scale, °R.
t_o = initial temperature, °R.
t_s = cylinder surface temperature, °R.
t_{sn} = temperature in the sheet at the nth level, °R.
t_{fn} = temperature in the felt at the nth level, °R.
t_a = air temperature, °R.
t_1 = initial average felt temperature, °R.
t_2 = final average felt temperature, °R.
t'_{so} = initial average sheet temperature, °R.
$\overline{t_l}$ = average temperature at which liquid is transferred to the felt, °R.
$\overline{u}$ = average velocity of liquid in a capillary, ft./hr.
V = velocity of sheet, ft./hr.
v = $H(dH)/(d\theta)$, sq.ft./hr.
X = thickness of sheet, ft.
x = distance through thickness of sheet, ft.
y = distance across width of sheet, ft.
z = distance along length of sheet, ft.

Greek Letters

α = thermal diffusivity, sq.ft./hr.
γ = surface tension, lb.$_{(f)}$/ft.
δ = thickness of felt, ft.
ϵ = emissivity, dimensionless
ξ = mass of moisture entering the felt, lb.$_m$/hr. sq.ft.
η = fraction of moisture entering the felt as a liquid, dimensionless
θ = time, hr.
Ψ = contact angle, radians
λ = latent heat of vaporization, B.t.u./lb.$_m$
ϕ = angle of inclination of capillary to the horizontal, radians
μ = viscosity, lb.$_m$/hr.-ft.
ρ = density, lb.$_m$/cu.ft.
σ = Stefan-Boltzmann constant, B.t.u./hr.-sq.ft.-°R.^{4}
τ_f = Fourier modulus based on felt properties, dimensionless
τ_s = Fourier modulus based on sheet properties, dimensionless

Subscripts

f = property of felt
s = property of sheet
x = property in the x direction
y = property in the y direction
z = property in the z direction

LITERATURE CITED

1. Bell, J. R., W. F. E. Robinson, and A. H. Nissan, *Tappi*, **40**, 558 (1957).
2. Brauns, O., and S. Ponton, *Svensk Papperstidning*, **62**, 245 (1959).
3. Carslaw, H. S., and J. C. Jaeger, "Conduction of Heat in Solids," 2 ed., Oxford Press, London, England (1959).
4. Nissan, A. H., *Tappi*, **37**, 597 (1954).
5. ———, and David Hansen, *A.I.Ch.E. Journal*, **6**, 606 (1960).
6. Nissan, A. H., and W. G. Kaye, *Tappi*, **38**, 385 (1955).
7. Palmer, W. B., *J. Textile Inst.*, **44**, T391 (1953).
8. Smith, S. F., and R. W. Atwood, *Tappi*, **36**, 481 (1953).

Manuscript received February 1, 1961; revision received April 19, 1961; paper accepted April 21, 1961. Paper presented at A.I.Ch.E. Cleveland meeting.

Energy Balances in Solar Distillers

G. O. G. LOF, J. A. EIBLING, and J. W. BLOEMER

Battelle Memorial Institute, Columbus, Ohio

There has been considerable doubt as to the manner in which the productivity of solar stills is affected by many of the designs and operating variables. To assist in designing solar stills of improved performance, theoretical equations are derived to describe the complete energy and mass transfer relationships involved in the operation of the basin type of solar still. These are supplemented with data from field operation of a 2,500-sq. ft. still. With these relationships and the aid of a digital computer, the effects of variations of design parameters on the performance of solar stills is predicted. Distiller productivity is correlated with atmospheric temperature, wind velocity, solar radiation, absorptivity and slope of transparent cover, and other variables. Curves showing the magnitude of the effects of design changes on cover temperature, brine temperature, and productivity are presented.

Although superficially a simple process the production of fresh water from sea water by solar distillation in basin types of distillers involves a complex set of operations comprising radiant and convective heat transfer, thermal conduction, vapor diffusion, evaporation and condensation, and other phenomena all taking place inside one piece of equipment. Even though the first practical solar distillation unit was built almost 90 yr. ago (2), a complete quantitative evaluation of these energy and mass transfer relationships has never been reported. The designing of this first

G. O. G. Lof is a consulting engineer in Denver, Colorado.